Modeling Molecular Weight Development of Gas-Phase α -Olefin Copolymerization

Tuyu Xie, Kim B. McAuley, James C. C. Hsu, and David W. Bacon
Dept. of Chemical Engineering, Queen's University, Kingston, Ontario, Canada K7L 3N6

A comprehensive kinetic model developed for molecular weight calculations of ethylene and α-olefin copolymerizations in the context of a terminal model accounts for multiple-type active centers of the catalyst, detailed elementary chemical reactions, and catalyst composition. The moments of copolymer chain distributions are defined considering molecular weights of comonomer units so that copolymer molecular weight averages can be directly calculated from those moments. A double Z-transformation is introduced for the derivation of differential equations of the moments. Model simulations are carried out based on ethylene and 1-butene copolymerizations in a gas-phase fluidized-bed reactor. Polydispersity of accumulated copolymer depends on catalyst composition and kinetic characteristics of the catalyst. For a catalyst with specified kinetic characteristics, the polydispersity depends on the mole fraction of each type of active center. For a catalyst with two types of active centers, the maximum polydispersity of copolymer occurs at 50 wt. % of the total copolymer if polydispersities of the copolymers generated at each active site are the same. Polydispersity of accumulated copolymer is sensitive to propagation reactions and chain transfer to hydrogen reactions. Differences in chain transfer to cocatalyst and monomers and in spontaneous deactivation rates for different types of active centers may play minor roles in controlling molecular weight development in the presence of hydrogen. This model can be used for catalyst composition design, simulation of commercial olefin copolymerization processes, and kinetic parameter estimation.

Introduction

Ethylene-based resins are the most prevalent commodity polymers, with current annual worldwide production of over 30 million ton. With improvements in both polymerization processes and catalysts, tremendous growth in the polyethylene industry continues in the 1990s. By 1995, the world demand for polyethylenes is projected to expand to more than 40 million ton/yr, and more than 25% of the total production will be produced using gas-phase processes (Payn, 1993). A distinguishing feature of gas-phase processes is that the polymerization zone does not involve any liquid phase. Thus, constraints due to liquid viscosity and solubility effects are eliminated, and so gas-phase processes provide more product flexibility compared with other conventional processes. Furthermore, the absence of solvent treatment reduces both plant construction and operation costs significantly. Gas-phase polymerization processes have been described in detail in comprehensive reviews by Short (1981), Choi and Ray (1985), and Xie et al. (1994). While gas-phase processes have been commercially successful, many fundamental issues involved in gas-phase polymerizations, such as molecular weight development of ethylene copolymers, have not been thoroughly studied. The present investigation was therefore designed to study molecular weight development of ethylene and α-olefin copolymerizations using heterogeneous transition metal catalysts in a gas-phase process.

Most commercial polyethylenes synthesized using transition metal catalysts are copolymers. One of the important features of ethylene and α-olefin copolymerizations using heterogeneous Ziegler-Natta catalysts is the broad molecular weight distribution (MWD) of the copolymer. Two theories have been developed to explain broad MWDs of polyethylenes, namely, the diffusion limitation theory and the multiple-type active-center theory. The former theory emphasizes

Present address of T. Xie: DuPont Canada Inc., Research & Development Center, Kingston, Ontario, Canada K7L 5A5.

the effect of monomer concentration on molecular weight development; the latter is more concerned with the influences of different types of active centers and associated kinetic parameters of MWD. However, recent modeling and experimental studies have suggested that the effect of monomer concentration due to diffusion limitations on MWD is negligible, and that characteristics of catalysts have a significant influence on MWD of polymer (Xie et al., 1994).

Assuming the polymer particles to be isothermal and spherical, Galvan and Tirrell (1986) developed a model for molecular weight calculation of olefin homopolymerization that accounted for two active sites and the limitation of monomer diffusion. Simulation results showed that the presence of different types of active sites is responsible for the broad MWD of olefin homopolymerization. Even when there are apparent monomer diffusion limitations, multiple active sites still play an important role in determining molecular weight development. Floyd et al. (1987; 1988) studied the effects of intraparticle and external boundary-layer transport resistances on kinetic behavior and polymer property development of olefin homopolymerization based on a multigrain model. It was found that diffusion resistances affect the polymerization rate more strongly than the molecular weights. Their simulation results showed that even in a highly diffusion-limited situation, the polydispersity drops below 4 within 30 min after polymerization begins. The simulation results by Galvan and Tirrell (1986) and Floyd et al. (1987; 1988) suggest that monomer concentration gradients in the macroparticle alone cannot explain the broad MWDs of polyethylenes produced under normal reactor operating conditions. The nature of the catalysts play a crucial role in controlling MWDs of polyethylenes. Hence, in recent modeling studies, emphasis has been focused on the effects of multiple types of active centers on MWD.

De Carvalho et al. (1989) developed a comprehensive ethylene and α-olefin copolymerization model that accounts for the formation, initiation, and deactivation of active centers, and for spontaneous chain transfer and chain transfer to hydrogen, monomer, and organometallics. This model shows that the instantaneous polydispersity for each active site equals 2 and that the instantaneous polydispersity for the entire amount of polymer produced deviates from 2 by the ratio of the variance of the propagation rate constant distribution to the mean propagation rate constant. The effect of the propagation rate constant distribution on molecular weight development was demonstrated by assuming unimodal and skewed bimodal distributions of propagation rate constants. The pseudokinetic rate constant method was used to evaluate the kinetic rate constants for each site. However, chain transfer reactions were not considered in the active center fraction calculations. Effects of chain transfer reactions on active center fraction calculations can be very important if chain transfer reactions are significant (Xie and Hamielec, 1993a,b,c).

Villermaux et al. (1989) and Lorenzini et al. (1991) developed a model for ethylene and 1-butene copolymerization with Ziegler-Natta catalyst at high temperature and high pressure. The model development was based on a single active site, which was then extended to two or three active sites using a mixing law. In their model development, the authors treated 1-butene as two units of ethylene. The moment equations were limited to chain-length calculations. Their model can be used for molecular weight calculations, but it is limited to the case of ethylene and 1-butene copolymerization. The polydispersity of polymer obtained for their system at high temperature and high pressure is between 3 and 5. It is worth noting that the polymerization occurs in a supercritical phase, the polymer being soluble in the monomer mixture. Therefore, there is no monomer diffusion limitation in this system. However, the polydispersity of polymer is similar to that obtained in a low temperature system. This suggests that multiple active sites play a central role in determining molecular weight development.

McAuley et al. (1990) developed a comprehensive model for gas-phase ethylene copolymerization in a fluidized bed reactor. Besides elementary reactions described by de Carvalho et al. (1989), the model also accounts for the effect of impurities on catalyst deactivation. This model can be used to predict average chain lengths for multiple-component copolymerization. The kinetic rate constants in each active site are expressed as pseudokinetic rate constants. The model was evaluated assuming two active-site types of catalyst.

Hutchinson et al. (1992) developed a detailed model for olefin copolymerization, accounting for mass and heat transfer, polymerization rate, molecular weights, and particle morphology development. Molecular weights of copolymer were calculated using average chain length multiplied by an average molecular weight of the monomers (McAuley et al., 1990; Hutchinson et al., 1992).

Although the importance of multiple types of active centers in controlling molecular weight development has been recognized, and significant modeling work has been published, only copolymer chain lengths have been calculated. These chain lengths are not equivalent to molecular weights for copolymers except for ideal alternating copolymer chains. Furthermore, the effect of each type of active center on MWD has not been comprehensively discussed in the literature. For example, what kinds of active centers will cause broad MWDs? What elementary chemical reactions are responsible for broad MWDs? What effect does the concentration level of each type of active center have on MWD? The purpose of the present investigation is to develop a comprehensive model for molecular weight calculations in α-olefin copolymerization that accounts for multiple active center types, detailed elementary chemical reactions, as well as composition of catalyst. Through simulations, this model is then used to study the effects of catalyst composition and elementary chemical reactions on molecular weight development for copolymers produced in a gas phase process.

Model Development

The chemical reactions of ethylene and α-olefin copolymerization, using heterogeneous Ziegler-Natta catalysts, can be envisioned as occurring at the interface between the solid catalyst and the polymer matrix, where the active centers are located. From gas-state monomer to solid-state polymer, ethylene and the comonomer experience a dramatic physicochemical transition within a very short time. The polymerization environment changes with the composition of the catalyst, polymerization process, reactant composition, reactor operating conditions, and extent of polymerization. Although

intensive research activity has been focused on Ziegler-Natta catalyst systems since their discovery in the early 1950s, no definitive, unequivocal chemical reaction mechanisms have been developed to fully describe the kinetic behavior of ethylene homo/copolymerizations, due to the complexity of the systems employed. Nevertheless, the key elementary chemical reactions have been established, which include formation of active centers, insertion of monomers into the growing polymer chains, chain transfer reactions, and catalyst deactivation. Most of the proposed mechanisms are based on information about polymerization rate, molecular weight and its distribution, polymer chain microstructure, and active center concentrations. Detailed mechanisms have been discussed in monographs (Boor, 1979; Kissin, 1985) and in reviews (Tait and Watkins, 1989; Dusseault and Hsu, 1993). Among the proposed propagation mechanisms, the one proposed by Cossee (Cossee, 1964; Arlman and Cossee, 1964) together with its subsequent modifications has been widely adopted. With Cossee's mechanism in mind, Bohm (1978) proposed perhaps the most comprehensive elementary chemical reactions involved in the ethylene polymerization process.

Since commercial production of linear low-density polyethylene (LLDPE) and high-density polyethylene (HDPE) consists of a copolymerization process, obviously copolymerization mechanisms are required to understand kinetic behavior and polymer properties. Therefore, Bohm's reaction model has been modified and extended to ethylene and α-olefin copolymerization processes in recent modeling studies (Villermaux et al., 1989; de Carvalho et al., 1989; McAuley et al., 1990; Lorenzini et al., 1991; Hutchinson et al., 1992). Furthermore, to illustrate multimodal distribution of the polymer chain composition and broad molecular weight distribution, the multiple-type active-center concept has been adopted in recent modeling studies. Therefore, a comprehen-

Table 1. Elementary Chemical Reactions of Ethylene and α-Olefin Copolymerization

Reaction			Description
Activation			
$C_p(j)$	$\xrightarrow{K_{as}(j)}$	$P_0^*(j)$	Spontaneous activation
$C_p(j)+[A]$	$\xrightarrow{K_{aA}(j)}$	$P_0^*(j)$	Activation by aluminum alkyl (A)
$C_p(j)+[H_2]$	$\xrightarrow{K_{aH}(j)}$	$P_0^*(j)$	Activation by hydrogen (H_2)
$C_p(j)+[M_1]$	$\xrightarrow{K_{aM1}(j)}$	$P_0^*(j)$	Activation by monomer 1 (M_1)
$C_p(j)+[M_2]$	$\xrightarrow{K_{aM2}(j)}$	$P_0^*(j)$	Activation by monomer 2 (M_2)
Initiation			
$P_0^*(j)+[M_1]$	$\xrightarrow{K_{i1}(j)}$	$P_{1,0,1}^*(j)$	Initiation of M_1 by normal active center
$P_0^*(j)+[M_2]$	$\xrightarrow{K_{i2}(j)}$	$P_{0,1,2}^*(j)$	Initiation of M_2 by normal active center
$P_{H,0}^*(j)+[M_1]$	$\xrightarrow{K_{iH1}(j)}$	$P_{1,0,1}^*(j)$	Initiation of M_1 by active center with H
$P_{H,0}^*(j)+[M_2]$	$\xrightarrow{K_{iH2}(j)}$	$P_{0,1,2}^*(j)$	Initiation of M_2 by active center with H
$P_{A,0}^*(j)+[M_1]$	$\xrightarrow{K_{iA1}(j)}$	$P_{1,0,1}^*(j)$	Initiation of M_1 by active center with A
$P_{A,0}^*(j)+[M_2]$	$\xrightarrow{K_{iA2}(j)}$	$P_{0,1,2}^*(j)$	Initiation of M_2 by active center with A
Propagation			
$P_{m,n,1}^*(j)+[M_1]$	$\xrightarrow{K_{11}(j)}$	$P_{m+1,n,1}^*(j)$	Propagation of chain type 1 with M_1
$P_{m,n,1}^*(j)+[M_2]$	$\xrightarrow{K_{12}(j)}$	$P_{m,n+1,2}^*(j)$	Propagation of chain type 1 with M_2
$P_{m,n,2}^*(j)+[M_1]$	$\xrightarrow{K_{21}(j)}$	$P_{m+1,n,1}^*(j)$	Propagation of chain type 2 with M_1
$P_{m,n,2}^*(j)+[M_2]$	$\xrightarrow{K_{22}(j)}$	$P_{m,n+1,2}^*(j)$	Propagation of chain type 2 with M_2
Chain Transfer			
$P_{m,n,i}^*(j)$	$\xrightarrow{K_{fspi}(j)}$	$P_0^*(j)+q_{m,n}(j)$	Spontaneous chain transfer or β-elimination
$P_{m,n,i}^*(j)+[H_2]$	$\xrightarrow{K_{fHi}(j)}$	$P_{H,0}^*(j)+q_{m,n}(j)$	Chain transfer to hydrogen (H_2)
$P_{m,n,i}^*(j)+[A]$	$\xrightarrow{K_{fAi}(j)}$	$p_{A,0}^*(j)+q_{m,n}(j)$	Chain transfer to aluminum alkyl (A)
$P_{m,n,i}^*(j)+[M_1]$	$\xrightarrow{K_{f1i}(j)}$	$P_{1,0,1}^*(j)+q_{m,n}(j)$	Chain transfer to M_1
$P_{m,n,i}^*(j)+[M_2]$	$\xrightarrow{K_{f2i}(j)}$	$P_{0,1,2}^*(j)+q_{m,n}(j)$	Chain transfer to M_2
Deactivation			
$P_{m,n,i}^*(j)$	$\xrightarrow{K_{dspi}(j)}$	$C_d(j)+q_{m,n}(j)$	Spontaneous deactivation
$P_{m,n,i}^*(j)+[Z]$	$\xrightarrow{K_{dZi}(j)}$	$C_d(j)+q_{m,n}(j)$	Deactivation by impurities or poison (Z)
$P_{m,n,i}^*(j)+[A]$	$\xrightarrow{K_{dAi}(j)}$	$C_d(j)+q_{m,n}(j)$	Deactivation by aluminum alkyl (A)
$P_{m,n,i}^*(j)+[H_2]$	$\xrightarrow{K_{dHi}(j)}$	$C_d(j)+q_{m,n}(j)$	Deactivation by hydrogen (H_2)
$P_{m,n,i}^*(j)+[M_1]$	$\xrightarrow{K_{dMi1}(j)}$	$C_d(j)+q_{m,n}(j)$	Deactivation by monomer 1
$P_{m,n,i}^*(j)+[M_2]$	$\xrightarrow{K_{dMi2}(j)}$	$C_d(j)+q_{m,n}(j)$	Deactivation by monomer 2

sive chemical reaction mechanism should include not only reactions proposed by Bohm (1978) but also reactions involving multiple components at different active-center types. Whether each type of active center has the same reaction mechanism is still uncertain at present. If one assumes that all of the active centers perform the same reaction mechanisms, but with different reaction rates for each elementary chemical reaction, then elementary chemical reactions that are used for the present modeling studies are summarized as in Table 1, where j indicates an active-center type. The terminal model is assumed to be valid for binary copolymerizations of olefins in the present modeling. However, if the penultimate model is valid for some systems, the mechanisms in Table 1 can be modified accordingly.

In the present modeling, a typical fluidized-bed reactor for gas phase ethylene and α-olefin copolymerization, such as UNIPOL (Xie et al., 1994), is considered. A well-mixed condition in the polymerization zone is assumed (McAuley et al., 1994). Therefore, the fluidized-bed reactor is treated as an ideal continuous stirred tank reactor (CSTR) for species population balances.

The moments for live and dead copolymer chain distributions are defined as follows (Ray et al., 1971; Xie and Hamielec, 1993a,b):

$$Y_{i,k}(j) = \sum_{m=0}^{\infty}\sum_{n=0}^{\infty}(mM_1 + nM_2)^k[P^*_{m,n,i}(j)] \qquad (i = 1, 2;\quad k = 0, 1, 2, \ldots) \quad (1)$$

$$Q_k(j) = \sum_{m=0}^{\infty}\sum_{n=0}^{\infty}(mM_1 + nM_2)^k[q_{m,n}(j)] \qquad (k = 0, 1, 2, \ldots) \quad (2)$$

where $Y_{i,k}(j)$ is the kth moment of live copolymer chains with terminal monomer type i produced at active centers of type j, and $Q_k(j)$ is the kth moment of dead copolymer chain distribution produced at active centers of type j. One can see that monomer molecular weights have been incorporated in the moment calculations. According to Eq. 2, the first moment of the dead copolymer chain distribution is the total weight of copolymer produced at active centers of type j. Therefore, based on this definition, both instantaneous and accumulated molecular weight averages of copolymer can be directly calculated using the moments. This method has not been used for olefin coordination copolymerizations prior to the present investigation.

On the basis of the elementary chemical reactions shown in Table 1, live and dead copolymer chain population balances for an ideal CSTR can be expressed as follows:

Active centers with chain length unity:

$$\frac{d([P^*_{1,0,1}(j)]V)}{Vdt} = \frac{[P^*_{1,0,1}(j)]_f V_f}{V} + R_{I1}(j) + \{K_{f11}(j)Y_{10}(j) + K_{f21}(j)Y_{20}(j) + K_{iH1}[P^*_{H,0}(j)] + K_{iA1}[P^*_{A,0}(j)]\}[M_1] - \Big\{K_{11}(j)[M_1] + K_{12}(j)[M_2] + K_{f11}(j)[M_1] + K_{f12}(j)[M_2] + K_{fH1}(j)[H_2] + K_{fA1}(j)[A] + K_{fsp1} + K_{dz1}(j)[Z] + K_{dH1}(j)[H_2] + K_{dA1}(j)[A] + K_{d11}(j)[M_1] + K_{d12}(j)[M_2] + K_{dsp1}(j) + \frac{1}{\theta}\Big\}[P^*_{1,0,1}(j)] \qquad (m = 1, n = 0) \quad (3)$$

$$\frac{d([P^*_{0,1,2}(j)]V)}{Vdt} = \frac{[P^*_{0,1,2}(j)]_f V_f}{V} + R_{I2}(j) + \{K_{f22}(j)Y_{20}(j) + K_{f12}(j)Y_{10}(j) + K_{iH2}[P^*_{H,0}(j)] + K_{iA2}[P^*_{A,0}(j)]\}[M_2] - \Big\{K_{22}(j)[M_2] + K_{21}(j)[M_1] + K_{f22}(j)[M_2] + K_{f21}(j)[M_1] + K_{fH2}(j)[H_2] + K_{fA2}(j)[A] + K_{fsp2} + K_{dz2}(j)[Z] + K_{dH2}(j)[H_2] + K_{dA2}(j)[A] + K_{d22}(j)[M_2] + K_{d21}(j)[M_1] + K_{dsp2}(j) + \frac{1}{\theta}\Big\}[P^*_{0,1,2}(j)] \qquad (m = 0,\quad n = 1). \quad (4)$$

Active centers with chain length $m + n \geq 2$:

$$\frac{d([P^*_{m,n,1}(j)]V)}{Vdt} = \frac{[P^*_{m,n,1}(j)]_f V_f}{V} + \{K_{11}(j)[P^*_{m-1,n,1}(j)] + K_{21}(j)[P^*_{m-1,n,2}(j)]\}[M_1] - \Big\{K_{11}(j)[M_1] + K_{12}(j)[M_2] + K_{f11}(j)[M_1] + K_{f12}(j)[M_2] + K_{fH1}(j)[H_2] + K_{fA1}(j)[A] + K_{fsp1} + K_{dz1}(j)[Z] + K_{dH1}(j)[H_2] + K_{dA1}(j)[A] + K_{d11}(j)[M_1] + K_{d12}(j)[M_2] + K_{dsp1}(j) + \frac{1}{\theta}\Big\}[P^*_{m,n,1}(j)] \quad (5)$$

$$\frac{d([P^*_{m,n,2}(j)]V)}{Vdt} = \frac{[P^*_{m,n,2}(j)]_f V_f}{V} + \{K_{12}(j)[P^*_{m,n-1,1}(j)] + K_{22}(j)[P^*_{m,n-1,2}(j)]\}[M_2] - \Big\{K_{21}(j)[M_1] + K_{22}(j)[M_2] + K_{f21}(j)[M_1] + K_{f22}(j)[M_2] + K_{fH2}(j)[H_2] + K_{fA2}(j)[A] + K_{fsp2} + K_{dz2}(j)[Z] + K_{dH2}(j)[H_2] + K_{dA2}(j)[A] + K_{d21}(j)[M_1] + K_{d22}(j)[M_2] + K_{dsp2}(j) + \frac{1}{\theta}\Big\}[P^*_{m,n,2}(j)]. \quad (6)$$

Dead polymer chains with chain length $m + n$:

$$\frac{d([q_{m,n}(j)]V)}{Vdt} = \frac{[q_{m,n}(j)]_f V_f}{V} + \{K_{f11}(j)[M_1] + K_{f12}(j)[M_2] + K_{fH1}(j)[H_2] + K_{fA1}(j)[A] + K_{fsp1}(j)\}[P^*_{m,n,1}(j)] + \{K_{f21}(j)[M_1] + K_{f22}(j)[M_2] + K_{fH2}(j)[H_2] + K_{fA2}(j)[A] + K_{fsp2}(j)\}[P^*_{m,n,2}(j)]$$

$$+\{K_{dz1}(j)[Z]+K_{dA1}(j)[A]+K_{dH1}(j)[H_2]+K_{d11}(j)[M_1]+K_{d12}(j)[M_2]+K_{dsp1}(j)\}[P^*_{m,n,1}(j)]+\{K_{dz2}(j)[Z]+K_{dH2}(j)[H_2]+K_{dA2}(j)[A]+K_{d21}(j)[M_1]+K_{d22}(j)[M_2]+K_{dsp2}(j)\}[P^*_{m,n,2}(j)]-\frac{[q_{m,n}(j)]}{\theta} \quad (7)$$

where θ is the average residence time of the polymer phase ($\theta = V/V_{out}$).

To simplify algebraic operations in deriving the moment equations, a double z-transformation is used involving the preceding chain-length balances and the definitions of moments. The double z-transformation of a function $g(m, n, t)$ is defined as

$$Z(z_1, z_2, t) = \sum_{m=0}^{\infty}\sum_{n=0}^{\infty} z_1^{-m} z_2^{-n} g(m, n, t) \quad (8)$$

where $g(m, n, t)$ is the concentration of live or dead copolymer chains in the present application. With the following transformations

$$z_1 = u^{-M_1}, \qquad z_2 = u^{-M_2} \quad (9)$$

Eq. 8 can be rewritten as the following generating functions:

$$f_i(u, t) = \sum_{m=0}^{\infty}\sum_{n=0}^{\infty} u^{(mM_1+nM_2)}[P^*_{m,n,i}(j)] \qquad (i=1,2) \quad (10)$$

$$f(u, t) = \sum_{m=0}^{\infty}\sum_{n=0}^{\infty} u^{(mM_1+nM_2)}[q_{m,n}(j)]. \quad (11)$$

Considering the definitions of moments in Eqs. 1 and 2, one can relate the moments of copolymer chain distribution to the generating functions as follows:

$$Y_{i0}(j) = f_i(u, t)|_{u=1} \qquad (i=1,2) \quad (12)$$

$$Y_{i1}(j) = \left(\frac{\partial f_i(u, t)}{\partial u}\right)\bigg|_{u=1} \qquad (i=1,2) \quad (13)$$

$$Y_{i2}(j) = \left(\frac{\partial^2 f_i(u, t)}{\partial u^2}\right)\bigg|_{u=1} + Y_{i1}(j) \qquad (i=1,2) \quad (14)$$

$$Q_0(j) = f(u, t)|_{u=1} \quad (15)$$

$$Q_1(j) = \left(\frac{\partial f(u, t)}{\partial u}\right)\bigg|_{u=1} \quad (16)$$

$$Q_2(j) = \left(\frac{\partial^2 f(u, t)}{\partial u^2}\right)\bigg|_{u=1} + Q_1(j). \quad (17)$$

Using Eqs. 3–7, 10, and 11, one can obtain generating functions for both live and dead copolymer chains. With Eqs. 12–17 and the resulting generating functions, the moment equations of polymer chain distribution can be derived as shown in the Appendix.

To solve the moments of copolymer chain distribution, one needs the following additional material balances:

Active centers formed by chain transfer to hydrogen:

$$\frac{d[P^*_{H,0}(j)]V}{Vdt} = \frac{[P^*_{H,0}(j)]_f V_f}{V} + \{K_{fH1}(j)Y_{10}(j) + K_{fH2}(j)Y_{20}(j)\}[H_2] - \left\{K_{iH1}(j)[M_1] + K_{iH2}(j)[M_2] + \frac{1}{\theta}\right\}[P^*_{H,0}(j)]. \quad (18)$$

Active centers formed by chain transfer to cocatalyst:

$$\frac{d[P^*_{A,0}(j)]V}{Vdt} = \frac{[P^*_{A,0}(j)]_f V_f}{V} + \{K_{fA1}(j)Y_{10}(j) + K_{fA2}(j)Y_{20}(j)\}[A] - \left\{K_{iA1}(j)[M_1] + K_{iA2}(j)[M_2] + \frac{1}{\theta}\right\}[P^*_{A,0}(j)]. \quad (19)$$

Total potential active centers:

$$\frac{d([C_p]V)}{Vdt} = \frac{[C_p]_f V_f}{V} - \sum_{j=1}^{N}\left\{K_{as}(j) + K_{aA}(j)[A] + K_{aH}(j)[H_2] + K_{aM1}(j)[M_1] + K_{aM2}(j)[M_2] + \frac{1}{\theta}\right\}F(j)[C_p]. \quad (20)$$

Initial active centers:

$$\frac{d([P^*_0(j)]V)}{Vdt} = \frac{[P^*_0(j)]_f V_f}{V} + \{K_{as}(j) + K_{aA}(j)[A] + K_{aH}(j)[H_2] + K_{aM1}(j)[M_1] + K_{aM2}(j)[M_2]\}[C_p(j)] - \left\{K_{iM1}(j)[M_1] + K_{iM2}(j)[M_2] + \frac{1}{\theta}\right\}[P^*_0(j)] \quad (21)$$

where $[C_p(j)] = F(j)[C_p]$.

Equations A1–A9 and 18–21 allow one to solve for the moments of dead copolymer chains produced at each active center type j. Thus, the molecular weight averages and polydispersity of the copolymer can be calculated as follows:

Instantaneous molecular weight averages of copolymer:

$$M_n = \frac{\sum_{j=1}^{N}\{dQ_1(j) + dY_{11}(j) + dY_{21}(j)\}}{\sum_{j=1}^{N}\{dQ_0(j) + dY_{10}(j) + dY_{20}(j)\}} \quad (22)$$

$$M_w = \frac{\sum_{j=1}^{N} \{dQ_2(j) + dY_{12}(j) + dY_{22}(j)\}}{\sum_{j=1}^{N} \{dQ_1(j) + dY_{11}(j) + dY_{21}(j)\}}. \quad (23)$$

Accumulated molecular weight averages of copolymer:

$$\bar{M}_n = \frac{\sum_{j=1}^{N} \{Q_1(j) + Y_{11}(j) + Y_{21}(j)\}}{\sum_{j=1}^{N} \{Q_0(j) + Y_{10}(j) + Y_{20}(j)\}} \quad (24)$$

$$\bar{M}_w = \frac{\sum_{j=1}^{N} \{Q_2(j) + Y_{12}(j) + Y_{22}(j)\}}{\sum_{j=1}^{N} \{Q_1(j) + Y_{11}(j) + Y_{21}(j)\}}. \quad (25)$$

Polydispersity of accumulated copolymer:

$$P_d = \frac{\left(\sum_{j=1}^{N} \{Q_2(j) + Y_{12}(j) + Y_{22}(j)\}\right)\left(\sum_{j=1}^{N} \{Q_0(j) + Y_{10}(j) + Y_{20}(j)\}\right)}{\left(\sum_{j=1}^{N} \{Q_1(j) + Y_{11}(j) + Y_{21}(j)\}\right)^2}. \quad (26)$$

Simulation Results and Discussion

In the present simulation, steady-state conditions for a single CSTR are assumed. The initiation rate for each type of active center j can be expressed by applying the stationary-state hypothesis (SSH) to Eq. 21 and by neglecting the effects of inflow and outflow on $P_0^*(j)$, that is,

$$R_I(j) = \{K_{as}(j) + K_{aA}(j)[A] + K_{aH}(j)[H_2] + K_{aM1}(j)[M_1] + K_{aM2}(j)[M_2]\}[C_p(j)]. \quad (27)$$

Hence,

$$R_{I1}(j) = \left(\frac{K_{iM1}(j)[M_1]}{K_{iM1}(j)[M_1] + K_{iM2}(j)[M_2]}\right) R_I(j) \quad (28)$$

$$R_{I2}(j) = \left(\frac{K_{iM2}(j)[M_2]}{K_{iM1}(j)[M_1] + K_{iM2}(j)[M_2]}\right) R_I(j) \quad (29)$$

At steady-state conditions, concentrations of monomers and hydrogen in the polymer matrix depend on reactor pressure, temperature, crystallinity of polymer chains, and physicochemical interaction between species and polymer. A detailed relationship accounting for all these factors has not been established. According to the recent study of Hutchinson and Ray (1990), low molecular weight hydrocarbon sorption in polyethylene can be expressed by Henry's law:

Table 2. Kinetic Parameters for Simulations of Ethylene and 1-Butene Copolymerization

Parameter	Active Center Type 1	Active Center Type 2	Units
$K_{11}(j)$	85.0	85.0	L/mol·s
$K_{12}(j)$	2.0	15.0	
$K_{21}(j)$	64.0	64.0	
$K_{22}(j)$	1.5	6.2	
$K_{f11}(j)$	0.0021	0.0021	L/mol·s
$K_{f12}(j)$	0.006	0.11	
$K_{f21}(j)$	0.0021	0.001	
$K_{f22}(j)$	0.006	0.11	
$K_{fH1}(j)$	0.088	0.37	
$K_{fH2}(j)$	0.088	0.37	
$K_{fA1}(j)$	0.024	0.12	
$K_{fA2}(j)$	0.048	0.24	
$K_{fsp1}(j)$	0.0001	0.0001	1/s
$K_{fsp2}(j)$	0.0001	0.0001	
$K_{dsp1}(j)$	0.0001	0.0001	1/s
$K_{dsp2}(j)$	0.0001	0.0001	

$$[M_i] = K_i^* P_i \quad (30)$$

where K_i^* can be calculated using the following correlation:

$$\log\{K_i^* \ (\text{mol}\cdot L^{-1}\cdot \text{atm}^{-1})\} = -2.38 + 1.08(T_c/T)^2. \quad (31)$$

Equations 30 and 31 are used for concentration calculations of ethylene and 1-butene at polymerization sites. Henry's law constant for hydrogen is estimated using the following correlation (Bohm, 1984):

$$\log\{K_H^* \ (\text{mol}\cdot L^{-1}\cdot \text{atm}^{-1})\} = -0.825 - 543/T. \quad (32)$$

For dynamic simulations, the total monomer mass balance for a fluidized-bed reactor has been developed (McAuley, 1991).

To study the effects of elementary chemical reactions at each type of active centers on molecular weight development of ethylene/α-olefin copolymers, we assume two types of active centers for the present simulations. The kinetic parameters for α-olefin copolymerization with different Ziegler-Natta catalysts may be different by orders of magnitude (Bohm, 1984; Kissin, 1985). The basic kinetic parameters used for the present simulations are listed in Table 2, where propagation-

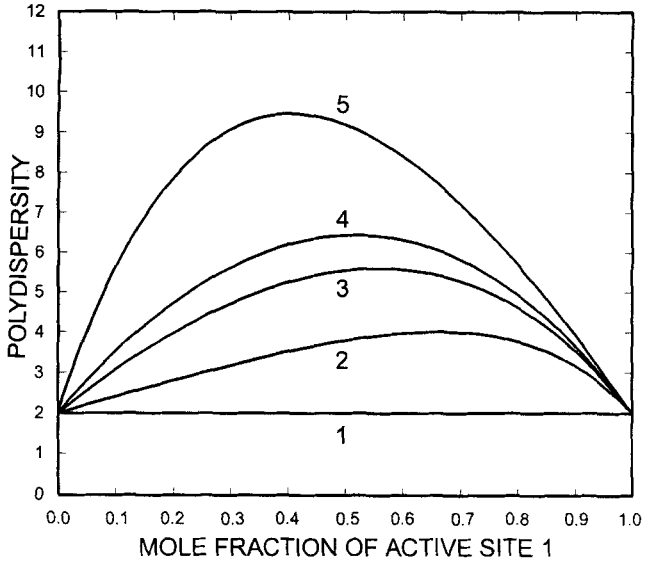

Figure 1. Dependence of polydispersity of copolymer on mole fraction of active center type 1.

1. $K_{ij}(2)/K_{ij}(1) = 10$; 2. $K_{ij}(2)/K_{ij}(1) = 2$; 3. Same as Table 2; 4. $K_{11}(2) = 100$, $K_{12}(2) = 1.5$, $K_{22}(2) = 1.1$, $K_{21}(2) = 14$; 5. $K_{11}(2) = 100$, $K_{12}(2) = 1.5$, $K_{22}(2) = 14$, $K_{21}(2) = 1.1$.

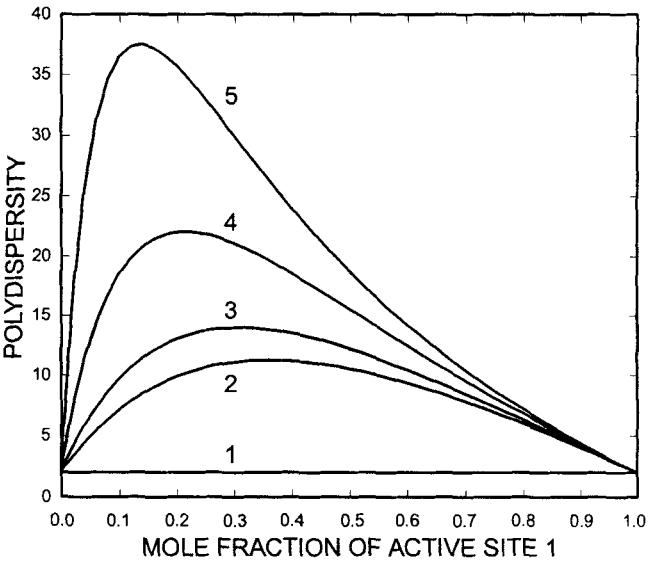

Figure 2. Dependence of polydispersity of copolymer on mole fraction of active center type 1.

1. Same as curve 1 in Figure 1; 2. $K_{22}(2) = 8.0$, $K_{21}(2) = 1.0$; 3. $K_{22}(2) = 1.0$, $K_{21}(2) = 1.0$; 4. $K_{22}(2) = 0.5$, $K_{21}(2) = 0.5$; 5. $K_{22}(2) = 0.25$, $K_{21}(2) = 0.25$; for all cases, $K_{11}(2) = 100$, $K_{12}(2) = 1.5$.

rate constants are based on data in the literature (Bohm, 1984; Kissin, 1985) and other parameters are arbitrary. Some parameters will be scaled to study the effects of elementary chemical reactions on the MWD of copolymer. Initiation-rate constants are assumed to be equal to propagation-rate constants. Spontaneous deactivation is effective and other deactivations are neglected in the model simulations. Ethylene and 1-butene are assigned as monomer 1 and monomer 2, respectively. Additional conditions are as follows:

[A]/[Ti]: 100
Ethylene: 77 mol% (in the gas phase)
1-Butene: 14%
Hydrogen: 9%
Residence time (polymer phase): 3.0 h
Reactor pressure: 22.0 atm

With these conditions, one can simulate the molecular weight development of ethylene and 1-butene copolymerization using different kinetic characteristics of the catalyst. The results are shown in Figures 1–13.

Figure 1 shows the polydispersity (P_d) of a copolymer changing with the mole fraction of each type of active center. Curve 3 was calculated using the parameters listed in Table 2. One can see that P_d of the copolymer is greater than 5 when the mole fraction of active-center type 1 is in the range of 0.4 to 0.7. For the same type of catalyst, P_d of the copolymer can be very different due to different relative quantities of the two active center types. Parameters used for the other curves in Figure 1 are the same as those for curve 1 except for the propagation rate constants for type 2 active centers. For curve 1, propagation rate constants for active-center type 2 are 10 times larger than those for the type-1 active center listed in Table 1. One can see that the polydispersity of copolymer hardly changes over the whole range of active-center mole fractions. This result suggests that multiple-type active centers may not always produce copolymers with broad MWD. Copolymers with narrow MWD may also be produced by catalysts with multiple active-center types, depending on the relative quantities of the different active-center types. If polymer chains produced at different active centers are similar in molecular weights, P_d of the accumulated copolymer would be small. For the case of curve 1, although propagation rate constants for type-2 active centers are 10 times larger than those for type 1 active centers, the polymer chains produced at active-center type 2 are not necessarily larger than those produced at active-center type 1 because chain transfer rate constants for active-center type 2 are much larger than those for active-center type 1. As a result, polymer chains produced at different active center types are similar in size. For curve 2, propagation-rate constants for active-center type 2 are two times larger than those for active-center type 1. Although still relatively small, P_d varies with the mole fraction of active-center type 1. In this case, polymer chains produced at different active center types are slightly different in size. Propagation-rate constants for active-center type 2 used for curve 4 are for ethylene and 1-butene copolymerization with a highly active Ziegler-Natta catalyst (Bohm, 1984). The maximum P_d is over 6 at 0.5 mol fraction of active-center type 1. With changing reactivity of active-center type 2, P_d of the copolymer changes significantly as shown in curve 5.

As $K_{22}(2)$ and $K_{21}(2)$ decrease, P_d increases dramatically, which can be seen in curves 2–5 of Figure 2. The maximum P_d is greater than 35 in the case of curve 5. However, even in the case of curve 5, P_d can be less than 5 if the mole fraction of active-center type 1 is larger than 0.9. Figures 2 and 3 suggest that catalysts with multiple-type active centers cannot be fully characterized by reactivities of each site type unless the relative quantities of each active-center type are also

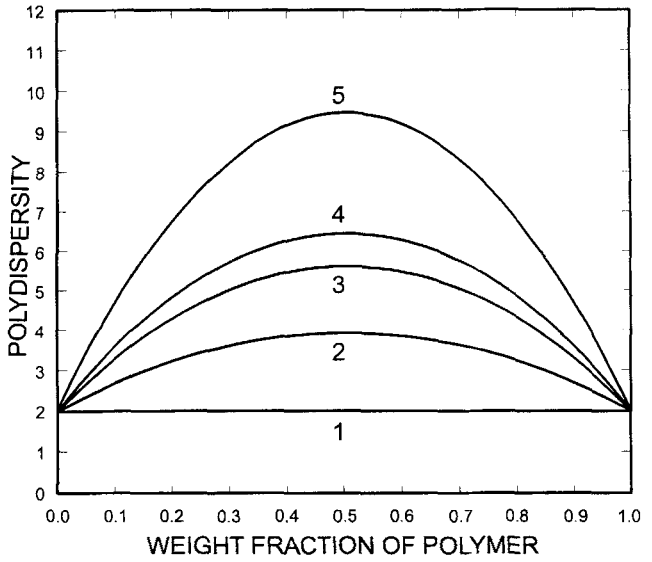

Figure 3. Dependence of polydispersity on weight fraction of copolymer produced at active center type 1.

Conditions are the same as those for Figure 1.

specified. This may be one of the main reasons why different catalyst preparation methods for the same family of catalysts can produce copolymers with very different MWDs. The relative fraction of each type of active center may depend on the history of catalyst preparation.

Figures 1 and 2 show that the P_d distribution is not symmetric with respect to the active-center type mole fraction for the parameters used in these simulations. But the P_d distribution is symmetric when plotted against the weight fraction of the copolymer produced by each type of active center, as shown in Figures 3 and 4. In general, the polydispersity of

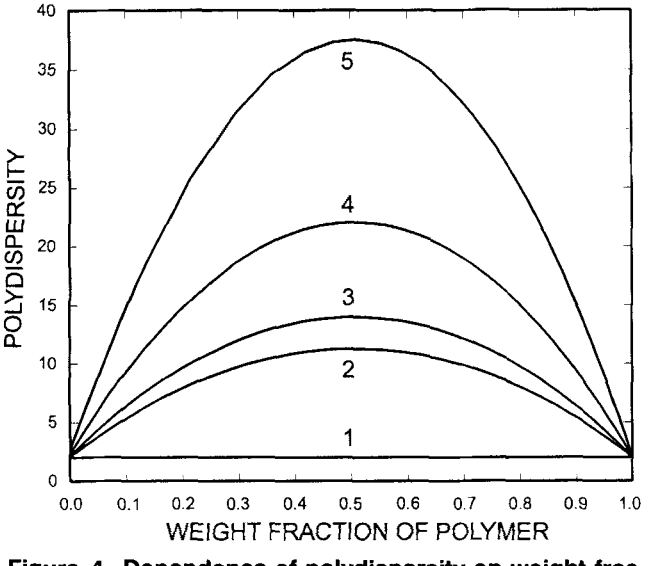

Figure 4. Dependence of polydispersity on weight fraction of copolymer produced at active center type 1.

Conditions are the same as those for Figure 2.

accumulated copolymer produced at different types of active centers can be expressed as a function of weight fraction, number average molecular weight, and polydispersity of polymer produced at each type of active center j as follows:

$$P_d = \left(\sum_{j=1}^{N} W(j)\overline{M}_n(j)P_d(j) \right) \left(\sum_{j=1}^{N} W(j)/\overline{M}_n(j) \right). \quad (33)$$

It should be pointed out that Eq. 33 is valid for polymers made using either a catalyst with multiple types of active centers or a mixture of catalysts. For a catalyst with two types of active centers ($N = 2$), differentiating Eq. 33 with respect to $W(1)$, which is the weight fraction of polymer produced at active center type 1, yields

$$\frac{dP_d}{dW(1)} = 2W(1)\left(P_d(1) - P_d(2)\frac{\overline{M}_n(2)}{\overline{M}_n(1)} - P_d(1)\frac{\overline{M}_n(1)}{\overline{M}_n(2)} + P_d(2) \right) + P_d(2)\frac{\overline{M}_n(2)}{\overline{M}_n(1)} + P_d(1)\frac{\overline{M}_n(1)}{\overline{M}_n(2)} - 2P_d(2). \quad (34)$$

Equation (34) allows one to solve for the weight fraction of the polymer produced at active-center type 1, at which maximum polydispersity is achieved, that is,

$$W(1) = \frac{2P_d(2) - P_d(2)\dfrac{\overline{M}_n(2)}{\overline{M}_n(1)} - P_d(1)\dfrac{\overline{M}_n(1)}{\overline{M}_n(2)}}{2\left(P_d(1) - P_d(2)\dfrac{\overline{M}_n(2)}{\overline{M}_n(1)} - P_d(1)\dfrac{\overline{M}_n(1)}{\overline{M}_n(2)} + P_d(2) \right)}. \quad (35)$$

From Eq. 35 it is clear that the maximum polydispersity occurs at weight fraction 0.5 of the total copolymer produced only if the polydispersities of copolymers produced at both types of active centers are the same. The polydispersity of copolymer produced at each active center is about 2 based on the present model calculations; hence, the maximum polydispersity of accumulated copolymer occurs at about 50 wt. % of the total copolymer produced, as shown in Figures 3 and 4. Equation 35 is in agreement with the results in Figures 3 and 4 and with the results of Floyd et al. (1987) for homopolymer. Equation 35 can also be used as a mixing law to determine weight fraction of polymer required to achieve maximum P_d, given the number average molecular weights and polydispersity of polymers produced by different catalysts. For example, a polymer produced using conventional heterogeneous Ziegler-Natta catalysts will have a polydispersity greater than 2, and a polymer made using metallocene-based catalysts will have a polydispersity of about 2. $W(1)$, the weight fraction of polymer produced by conventional Ziegler-Natta catalyst, must then be less than 0.5 to achieve maximum P_d if a polymer is produced using a mixture of these catalysts. Metallocene-based catalysts may soon be commercialized for gas or slurry processes (Xie et al., 1994).

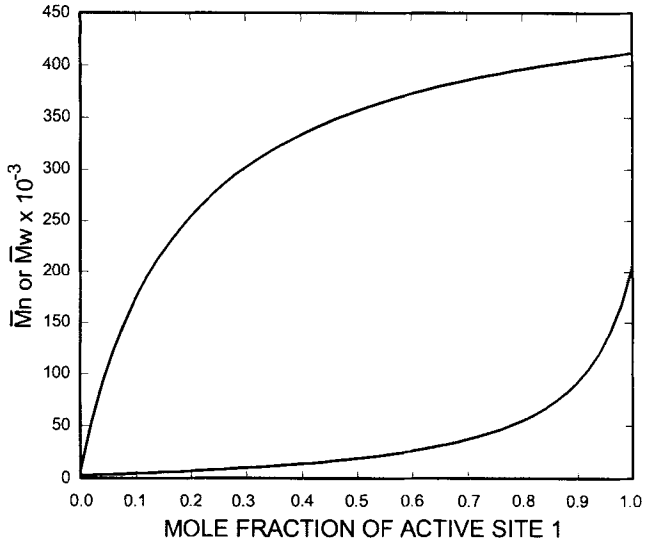

Figure 5. Dependence of molecular weight on mole fraction of active center type 1.

Parameters are the same as those for curve 5 in Figure 2.

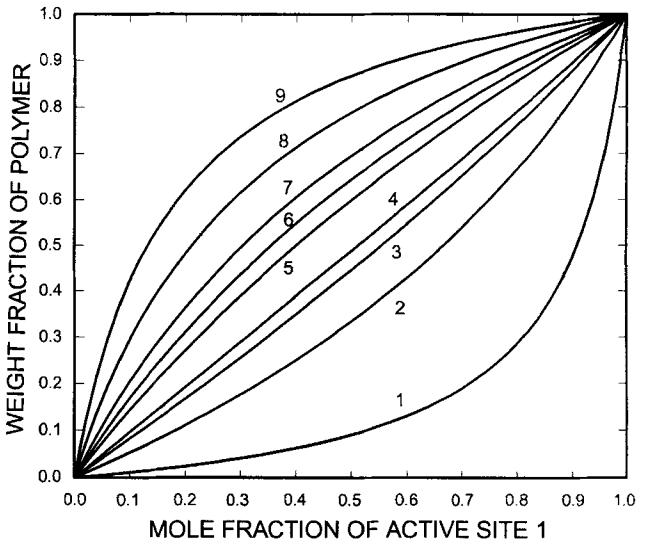

Figure 6. Relationships between mole fraction of active center type 1 and weight fraction of polymer produced by this active center type.

Parameters for curves 1–5 are the same as those for curves 1–5 in Figure 1 and parameters for curves 6–9 are the same as those for curves 2–5 in Figure 2, respectively.

One route to commercialization of metallocene-based catalysts for gas phase or slurry processes is to combine metallocene-based catalysts with conventional Ziegler-Natta catalysts. Fries and Bowles (1993) showed that combining a metallocene catalyst [$P_d(1) = 2.2$] and a conventional Ziegler-Natta catalyst [$P_d(2) = 8.0$, which can be understood as a composite site] can produce polyethylene with polydispersities in the range of 13.5 to 57.8, depending on the particular combination of these two catalysts. Assuming metallocene catalyst as a single active site and conventional Ziegler-Natta catalyst as multiple-type active centers, one can use the present model to design a mixed catalyst composition to produce a copolymer with the desired polydispersity.

For two active center types or two types of catalysts with the same polydispersity [$P_d(1) = P_d(2)$] of polymer, one can obtain the maximum polydispersity by substituting $W(1) = W(2) = 0.5$ into Eq. 33 and letting $N = 2$,

$$P_{d\max} = \left(\frac{0.25 P_d(1)\overline{M}_n(1)}{\overline{M}_n(2)}\right)\left(1 + \frac{\overline{M}_n(2)}{\overline{M}_n(1)}\right)^2. \qquad (36)$$

This equation shows that the number-average molecular weights produced by the two types of active centers must differ by at least an order of magnitude to achieve maximum polydispersity greater than 6 if $P_d(1) = P_d(2) = 2$. Figure 5 shows a typical molecular weight development for a catalyst with two types of active centers. The parameters for Figure 5 are the same as those used for curve 5 in Figure 2. In Figure 5 $\overline{M}_n(1)$ is about 73 times larger than $\overline{M}_n(2)$. This is because chain transfer rate constants for active-center type 2 are higher than those for active-center type 1 and propagation rate constants for growing chains with terminal monomer 2 at active center type 2 are smaller than those at active center type 1. As a result, the maximum polydispersity at $W(1) = W(2) = 0.5$ is about 37.5 as shown in Figure 2 (curve 5). Hence the present model calculation is in agreement with Eq. 36.

The concept of multiple active centers can be extended to multiple catalysts, particularly metallocene-based catalysts. Metallocene-based catalysts, such as titanocene, zirconocene, and hafnocene catalysts, yield polyethylenes with a polydispersity of about 2. However, mixtures of the metallocene catalysts produce polyethylenes with polydispersities up to about 10 (Ahlers and Kaminsky, 1988; Heiland and Kaminsky, 1992). The present model calculations are consistent with these experimental findings and the model can be used for designing catalyst mixtures to achieve the desired polydispersity of olefin copolymers.

Figure 6 shows the relationships between mole fraction of active center type 1 and the weight fraction of polymer produced by this type of active center. These curves allow one to determine the mole fraction of each type of active center required to produce a specified weight fraction of copolymer. A catalyst with a mixture of active center mole fractions corresponding to 0.5 weight fraction of copolymer will produce polyethylene with maximum polydispersity. Figure 6 also demonstrates that polydispersity is not symmetric with respect to mole fraction of active-center type 1.

Figures 1 and 2 show that the polydispersity of a copolymer depends on the combination of active-center types with different chemical properties. However, these calculations do not show the effect of individual elementary chemical reactions on polydispersity. To study the effect of individual elementary chemical reactions on P_d, all the parameters for two types of active centers are assumed to be the same except for the chemical reaction under consideration. Figure 7 shows the effect of the spontaneous deactivation rate of active-center type 2 on polydispersity of accumulated copolymer. All the other parameters are the same as those for active-center type 1 listed in Table 1, and the only difference between the two types of active centers is in deactivation rate constants. If the difference in deactivation rate constants between the two

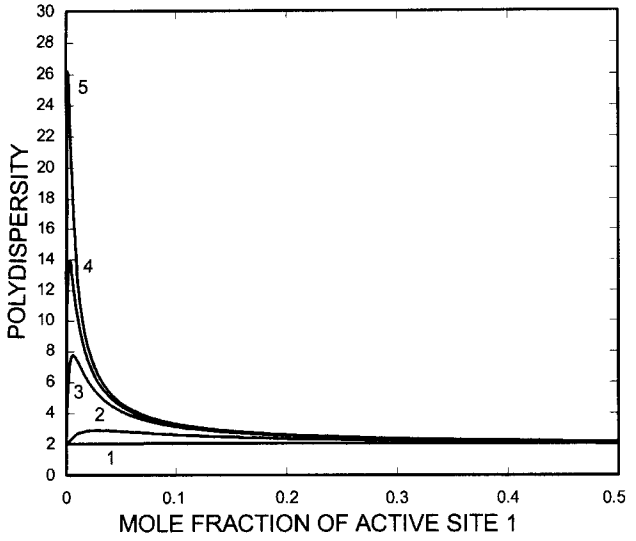

Figure 7. Effect of spontaneous deactivation reaction on polydispersity.

$K_{dspi}(2)/K_{dspi}(1)$: 1. 10; 2. 100; 3. 500; 4. 1,000; 5. 2,000.

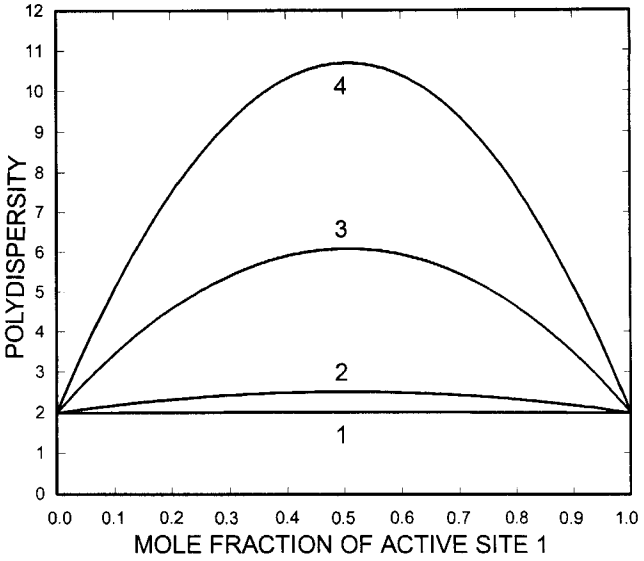

Figure 9. Effects of chain transfer to hydrogen rate constants on polydispersity.

$K_{fHi}(2)/K_{fHi}(1)$: 1. 2; 2. 10; 3. 50; 4. 100.

types of active centers is less than two orders of magnitude, polydispersity is not sensitive to deactivation rate constants, as shown in curves 1 and 2. However, if the difference between the deactivation rate constants for the two active-center types is over three orders of magnitude, polyethylene with large P_d is produced, as shown in curves 4 and 5. If the mole fraction of active-center type 1 is greater than 0.1, P_d is still small even for curves 4 and 5. In this case, the polymer is mainly produced at active-center type 1; hence, the effect of active-center type 2 is small. Figure 8 shows a local view of the range of mole fractions of active-center type 1 at which a polymer with a broad MWD will be produced. One can see

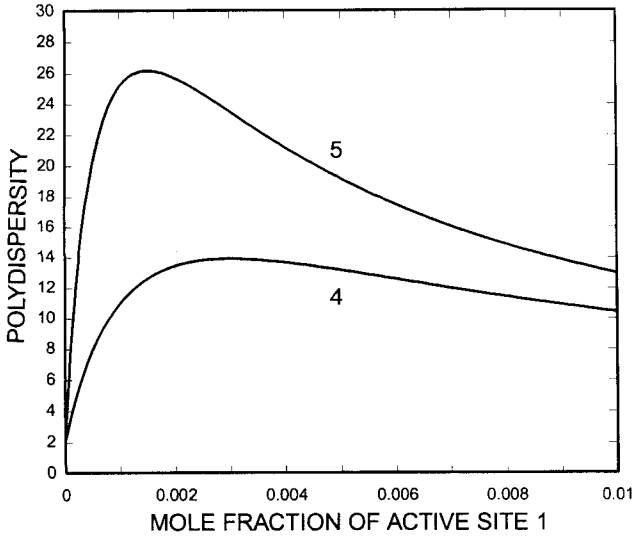

Figure 8. Effect of spontaneous deactivation reaction on polydispersity.

Conditions are the same as those for curves 4 and 5 in Figure 7.

that active-center type 2 dominates the composition of the catalyst to produce a copolymer with a large polydispersity for the case of curves 4 and 5. A catalyst with such high deactivation rate constants, compared with propagation rate constants, cannot have high productivity. Therefore, differences in deactivation rate constants cannot be the main reason for a broad MWD resulting from a high productivity catalyst in the presence of hydrogen.

Figure 9 shows the effects of chain transfer to hydrogen rate constants on polydispersity. One can see that polydispersity is not sensitive to chain transfer to hydrogen if the chain transfer to hydrogen rate constants differ by less than an order of magnitude. However, if the chain transfer to hydrogen rate constants differ by two orders of magnitude, polymer with broad MWD will be produced according to the present simulations, as shown in curve 4. It is assumed that the reactivity of the active centers formed by chain transfer to hydrogen is the same as those of normal active centers. Therefore, the polymerization rate will not be changed due to chain transfer to hydrogen. Thus, each type of active center produces the same amount of polymer because the propagation rate constants for both active center types are the same and the maximum polydispersity occurs at a site mole fraction of 0.5. However, if the active centers formed by chain transfer to hydrogen are different from normal active centers, then each type of active center will produce a different amount of polymer at a site mole fraction of 0.5. According to a recent experimental study for gas phase ethylene polymerization (Salajka et al., 1993), hydrogen reduces the polymerization rate significantly. Jaber and Ray (1993), however, showed that hydrogen enhances the polymerization rate at moderate concentration, but that a high concentration of hydrogen results in a decreasing rate of ethylene copolymerization in a solution process. This suggests that hydrogen may play other roles than that of a chain transfer agent. Nevertheless, in the presence of hydrogen, the main chain transfer process is domi-

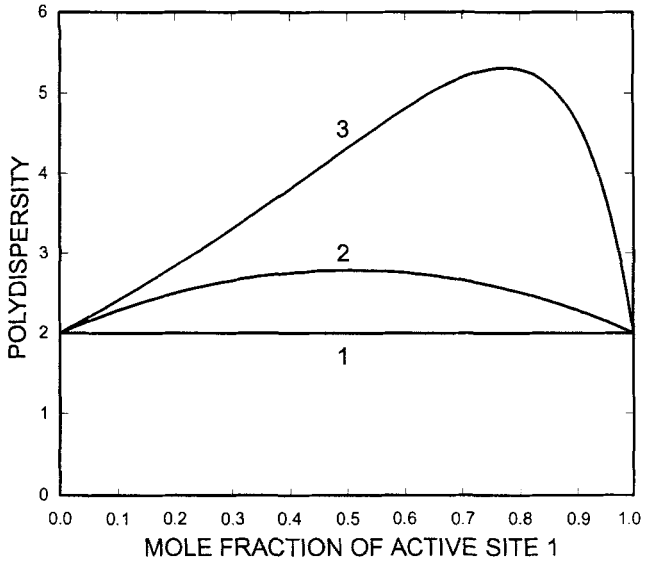

Figure 10. Effects of chain transfer to cocatalyst rate constants on polydispersity.

$K_{fAi}(2)/K_{fAi}(1)$: 1. 10; 2. 100; 3. 1000.

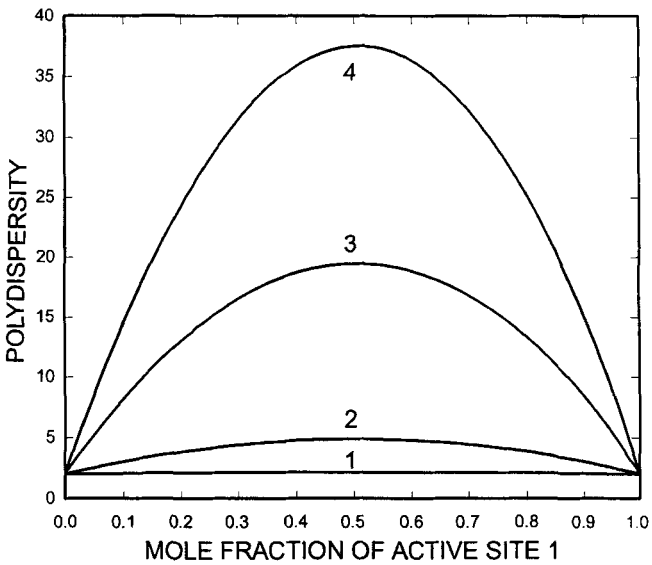

Figure 11. Effects of chain transfer to monomer rate constants on polydispersity.

$K_{fij}(2)/K_{fij}(1)$: 1. 2; 2. 10; 3. 50; 4. 100.

nated by chain transfer with hydrogen (Marques et al., 1993). Hence, differences in chain transfer to hydrogen rate constants between two active center types may play an important role in determining the MWD of a copolymer.

Figure 10 shows effects of chain transfer to cocatalyst rate constants on polydispersity. One can see that polydispersity is hardly changed if the chain transfer to cocatalyst rate constants differ by less than two orders of magnitude. When the ratio of $K_{fAi}(2)/K_{fAi}(1)$ is over three orders of magnitude, the maximum polydispersity is over 5, as shown in curve 3. However, $K_{fAi}(2)$ would need to be extremely high to produce polymer with broad MWD. Such a high $K_{fAi}(2)$ is not realistic because the molecular weight of polyethylene in general is not very sensitive to the concentration of cocatalyst, although the molecular weight decreases with an increase in the concentration of cocatalyst (Marques et al., 1993). Therefore, differences in chain transfer to cocatalyst rate constants may not be a main reason for broad MWD of copolymer.

The effects of chain transfer to monomer rate constants on polydispersity are shown in Figure 11. If the chain transfer to monomer rate constants for the two types of active center differ by more than an order of magnitude, polydispersity is very sensitive to the chain transfer to monomer rate constants. It should be mentioned that chain transfer to hydrogen is neglected for this simulation. Otherwise, molecular weight is always controlled by chain transfer to hydrogen (Marques et al., 1993). Furthermore, chain transfer to monomer rate constants depend very much on monomer properties. For the same monomer, it is not clear why different active centers could have different chain transfer to monomer reactivity. Nevertheless, differences in chain transfer to monomer rate constants between different active center types could be significant in causing broad MWD of a copolymer if hydrogen is absent.

Figure 12 shows the effects of propagation rate constants on polydispersity. All the parameters for both active-center types are the same as those for active-center type 1 listed in Table 2, except for the propagation rate constants for active-center type 2. The propagation rate constants for active-center type 2 used for curve 1 are ideal, that is $r_1 r_2 = 1$. Under this condition, type 2 active centers show the same preference for adding one or the other of the two monomers regardless of terminal monomer type. One can see from curve 1 that polydispersity is independent of a mole fraction of the active center type. Propagation rate constants for active-center type 2

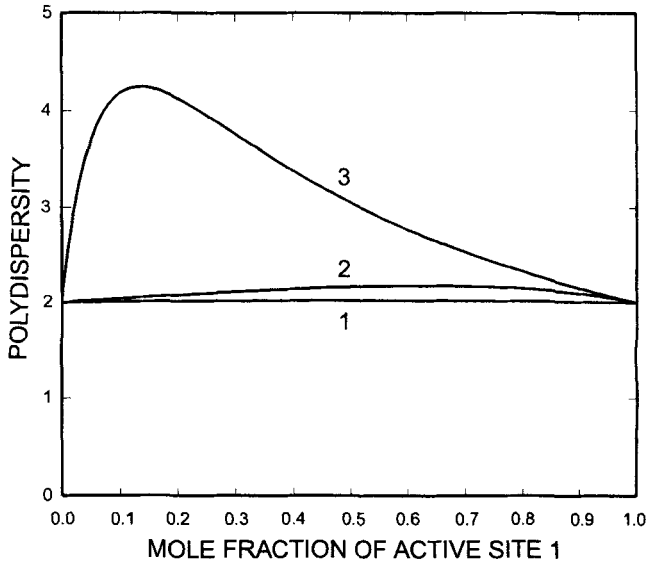

Figure 12. Effects of propagation rate constants on polydispersity.

$K_{ij}(1)$ are the same as those listed in Table 1. 1. $K_{11}(2) = K_{21}(2) = 100$, $K_{12}(2) = K_{22}(2) = 4$; 2. $K_{11}(2) = K_{22}(2) = 0.01$, $K_{12}(2) = K_{21}(2) = 100$; 3. $K_{11}(2) = 100$, $K_{12}(2) = 1.5$, $K_{22}(2) = K_{21}(2) = 0.25$.

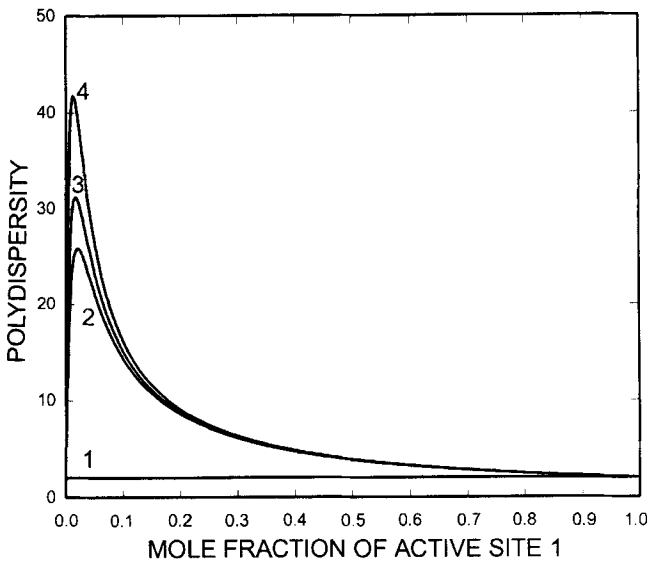

Figure 13. Effects of propagation rate constants on polydispersity.

$K_{ij}(1)$ are the same as those listed in Table 1. 1. $K_{11}(2) = 100$, $K_{21}(2) = 2$, $K_{12}(2) = 50$, $K_{22}(2) = 3$; 2. $K_{11}(2) = 100$, $K_{22}(2) = 50$, $K_{12}(2) = K_{21}(2) = 0.25$; 3. $K_{11}(2) = K_{12}(2) = 0.25$, $K_{22}(2) = 50$, $K_{21}(2) = 100$, 4. $K_{11}(2) = 100$, $K_{22}(2) = 50$, $K_{12}(2) = K_{21}(2) = 0.15$.

for curve 2 are close to alternating copolymerization conditions: $r_1 = r_2 \cong 0$. Polydispersity changes slightly with changes in catalyst site fractions as shown in curve 2. Propagation rate constants for active centers of type 2 on curve 3 are only active when the terminal unit of the active-center is monomer 1. One can see that the polydispersity is sensitive to the mole fractions of the active centers.

Figure 13 shows further effects of propagation rate constants on polydispersity. In curve 1, both r_1 and r_2 for active-center type 2 are much greater than unity (therefore, $r_1 r_2 \geq 1$); hence, there is a tendency to form a block copolymer at active-center type 2. However, polydispersity is still independent of composition of active-center type 2. Curves 2–4 show significant changes in polydispersity with propagation rate constants for active-center type 2. A common characteristic of these propagation rate constants is that the active center of type 2 is only active with a certain terminal monomer. When the terminal monomer is another type of monomer, the reactivity of this active center is reduced dramatically. In other words, one of the monomers is an inhibitor for this type of active center. A combination of this kind of active center type with a normal active center as shown in Table 2 for site 1 will lead to copolymer with broad MWD. Again, a polymer with a high polydispersity can be produced only with a certain composition of catalyst, as shown in Figure 13. Figures 12 and 13 suggest that differences in propagation rate constants between two types of active centers may be one of the main reasons for the broad MWD of polymer produced using heterogeneous Ziegler-Natta catalysts, although in some cases the differences in propagation rate constants will not affect the polydispersity of copolymer.

As mentioned earlier, the kinetic parameters used for the present simulations are arbitrary, particularly for the simulations of the effects of individual elementary chemical reactions on MWD. However, these simulations do indicate the trends in the effects of different types of active centers on MWDs of α-olefin copolymers produced using heterogeneous Ziegler-Natta catalysts. The model simulations also suggest that it is important and challenging to determine the kinetic parameters for each type of active center as well as the site type distribution of the catalyst. It should also be mentioned that the simulation results shown in this work are limited to the situations of the parameters used. It is crucial for simulating commercial polymerization processes and product quality control to obtain accurate kinetic parameters. This can only be done through a combination of comprehensive modeling and well-designed experiments. Systematic experimental studies of ethylene and α-olefin copolymerizations in a gas phase process are being conducted in the authors' laboratory.

Conclusions

A comprehensive model for molecular weight calculations in olefin copolymerizations has been developed that accounts for multiple types of active centers, detailed elementary chemical reactions, and mole fractions of individual sites on the catalyst. The simulation results show that the polydispersity of an accumulated polymer depends on catalyst composition and the characteristics of each type of active center. However, a catalyst with multiple types of active centers may not produce a copolymer with a broad MWD if the polymer chains generated at each type of active center are similar in size. The maximum polydispersity depends on the mole fractions of site types on the catalyst for given kinetic characteristics of the catalyst. For a catalyst with two types of active centers, the maximum polydispersity occurs at 50 wt. % of total polymer produced if the polydispersity of the polymer produced by each type of active center is the same. Polydispersity of accumulated copolymer depends on the elementary chemical reactions at each type of active center. According to the present simulations, differences in propagation and chain transfer to hydrogen rate constants between different types of active centers can play an important role for broad MWD of copolymers. Differences in deactivation rate constants and in chain transfer to cocatalyst and monomer rate constants appear to play only a minor role in controlling the MWD of the copolymer; however, these reactions could be significant when hydrogen is absent. The present model can be used for designing the compositions of conventional Ziegler-Natta or metallocene-based catalysts to achieve products with the desired polydispersity, for simulating commercial olefin copolymerization processes, and for estimating kinetic parameters from valid experimental data.

Acknowledgment

Financial support from The Manufacturing Research Corporation of Ontario is gratefully acknowledged.

Notation

$[A]$ = concentration of cocatalyst, mol/L
$[C_d]$ = concentration of dead centers, mol/L
$[C_p(j)]$ = concentration of potential active center type j, mol/L
$F(j)$ = mole fraction of active center type j

F_{Hf} = feed rate of hydrogen, mol/s
F_{Mif} = feed rate of monomer i ($i = 1, 2$), mol/s
$[H_2]$ = concentration of hydrogen, mol/L
i = monomer type
$K_{ik}(j)$ = propagation rate constant of active-center type j with terminal monomer i adding another monomer k ($i = 1, 2$; $k = 1, 2$), L/mol·s
$K_{as}(j)$ = spontaneous activation rate constant of active-center type j, 1/s
$K_{aA}(j)$ = activation rate constant of active-center type j by cocatalyst, L/(mol·s)
$K_{aH}(j)$ = activation rate constant of active-center type j by hydrogen, L/(mol·s)
$K_{aMi}(j)$ = activation rate constant of active-center type j by monomer i ($i = 1, 2$), L/(mol·s)
$K_{fik}(j)$ = chain transfer rate constant of active-center type j with terminal monomer i transferring to monomer k ($i = 1, 2$; $k = 1, 2$), L/(mol·s)
$K_{fAi}(j)$ = chain transfer rate constant of active-center type j with terminal monomer i ($i = 1, 2$) transferring to cocatalyst, L/(mol·s)
$K_{fHi}(j)$ = chain transfer rate constant of active-center type j with terminal monomer i ($i = 1, 2$) transferring to hydrogen, L/(mol·s)
$K_{fspi}(j)$ = spontaneous chain transfer rate constant of active-center type j with terminal monomer i ($i = 1, 2$), 1/s
$K_{dspi}(j)$ = spontaneous deactivation rate constant of active-center type j, 1/s
$K_{dAi}(j)$ = deactivation rate constant of active-center type j with terminal monomer i ($i = 1, 2$) by cocatalyst, L/(mol·s)
$K_{dHi}(j)$ = deactivation rate constant of active-center type j with terminal monomer i ($i = 1, 2$) by hydrogen, L/(mol·s)
$K_{dMik}(j)$ = deactivation rate constant of active-center type j with terminal monomer i ($i = 1, 2$) by monomer k ($k = 1, 2$), L/(mol·s)
$K_{dZi}(j)$ = deactivation rate constant of active-center type j with terminal monomer i ($i = 1, 2$) by impurities, L/(mol·s)
$K_{iAi}(j)$ = initiation rate constant of monomer i by active center j formed by chain transfer to cocatalyst, L/(mol·s)
$K_{iHi}(j)$ = initiation rate constant of monomer i by active center j formed by chain transfer to hydrogen, L/mol·s
$K_{iMi}(j)$ = initiation rate constant of monomer i by active center j, L/mol·s
m = number of units of monomer 1 bound in copolymer chain
M_i = molecular weight of monomer i ($i = 1, 2$)
$[M_i]$ = concentration of monomer i ($i = 1, 2$), mol/L
$\overline{M}_n(j)$ = accumulated number-average molecular weight of polymer produced at active center type j
$\overline{M}_w(j)$ = accumulated weight-average molecular weight of a polymer produced at active center type j
n = number of units of monomer 2 bound in copolymer chain
$[P^*_{A,0}(j)]$ = concentration of active center type j formed by chain transfer to cocatalyst, mol/L
P_i = partial pressure of species i, atm
r_1, r_2 = reactivity ratios of an active center with terminal monomer 1 and 2, respectively
$R_{fmi}(j)$ = reaction rate of chain transfer to monomer i, mol/(L·s)
R_I = total initiation rate, mol/(L·s)
$R_{Ii}(j)$ = initiation rate of monomer i by active center type j, mol/(L·s)
$R_{iHA1}(j)$ = initiation rate of monomer 1 by $P^*_{H,0}(j)$ and $P^*_{A,0}(j)$, mol/(L·s)
$R_{iHA2}(j)$ = initiation rate of monomer 2 by $P^*_{H,0}(j)$ and $P^*_{A,0}(j)$, mol/(L·s)
R_{p1} = polymerization rate of monomer 1, mol/(L·s)
R_{p2} = polymerization rate of monomer 2, mol/(L·s)
t = polymerization time, s
T = polymerization temperature, K
T_c = critical temperature of species i, K
$[T_i]$ = concentration of titanium, mol/(L·s)
u = a parameter defined in Eq. 9
V = volume of polymer phase, L
V_f = volumetric feed rate, L/s
V_{out} = volumetric outflow rate, L/s
z_i = variables defined in Eq. 8
$[Z]$ = concentration of impurity, mole/L

Literature Cited

Ahlers, A., and W. Kaminsky, "Variation of Molecular Weight Distribution of Polyethylenes Obtained with Homogeneous Ziegler-Natta Catalysts," *Makromol. Chem. Rapid Commun.*, **9**, 457 (1988).

Arlman, E. J., and P. Cossee, "Ziegler-Natta Catalysis III. Stereospecific Polymerization of Propene with the Catalyst System $TiCl_3$-$AlEt_3$," *J. Catal.*, **3**, 99 (1964).

Bohm, L. L., "Homo- and Copolymerization with a Highly Active Ziegler-Natta Catalyst," *J. Appl. Poly. Sci.*, **29**, 279 (1984).

Bohm, L. L., "Reaction Model for Ziegler-Natta Polymerization," *Polymer*, **19**, 545 (1978).

Boor, J., Jr., *Ziegler-Natta Catalysts and Polymerizations*, Academic Press, New York (1979).

Choi, K. Y., and W. H. Ray, "Recent Developments in Transition Metal Catalyzed Olefin Polymerization—A Survey I. Ethylene Polymerization," *J. Macromol. Sci. Rev. Macromol. Chem. Phys.*, **C25**, 1 (1985).

Cossee, P., "Ziegler-Natta Catalysts 1. Mechanism of Polymerization of α-Olefin with Ziegler-Natta Catalysts," *J. Catal.*, **3**, 80 (1964).

De Carvalho, A. B. M., P. E. Gloor, and A. E. Hamielec, "A Kinetic Mathematical Model for Heterogeneous Ziegler-Natta Copolymerization," *Polymer*, **30**, 280 (1989).

Dusseault, J. J. A., and C. C. Hsu, "$MgCl_2$ Supported Ziegler-Natta Catalysts for Olefin Polymerization: Basic Structure, Mechanism and Kinetic Behavior," *J. Macromol. Sci. Rev., Macromol. Chem. Phys.*, **C33**, 103 (1993).

Floyd, S., T. Heiskanen, T. W. Taylor, G. E. Mann, and W. H. Ray, "Polymerization of Olefins through Heterogeneous Catalysis VI. Effect of Particle Heat and Mass Transfer on Polymerization Behaviour and Polymer Properties," *J. Appl. Poly. Sci.*, **33**, 1021 (1987).

Floyd, S., T. Heiskanen, and W. H. Ray, "Solid Catalyzed Olefin Polymerization," *Chem. Eng. Prog.*, 56 (Nov., 1988).

Fries, R. W., and W. A. Bowles, "Organometallic Modified Polyolefin Catalysts for Enhanced Molecular Properties," *Metcon'93*, Houston (1993).

Galvan, R., and M. Tirrel, "Molecular Weight Distribution Predictions for Heterogeneous Ziegler-Natta Polymerization Using a Two-Site Model," *Chem. Eng. Sci.*, **41**, 2385 (1986).

Heiland, K., and W. Kaminsky, "Comparison of Zirconocene and Hafnocene Catalysts for the Polymerization of Ethylene and 1-Butene," *Makromol. Chem.*, **193**, 601 (1992).

Hutchinson, R. A., and W. H. Ray, "Polymerization of Olefins Through Heterogeneous Catalysis VIII. Monomer Sorption Effects," *J. Appl. Poly. Sci.*, **41**, 51 (1990).

Hutchinson, R. A., C. M. Chen, and W. H. Ray, "Polymerization of Olefins Through Heterogeneous Catalysis X. Modelling of Particle Growth and Morphology," *J. Appl. Poly. Sci.*, **44**, 1389 (1992).

Jaber, I. A., and W. H. Ray, "Polymerization of Olefins through Heterogeneous Catalysts: XII. The Influence of Hydrogen in the Solution Copolymerization of Ethylene," *J. Appl. Poly. Sci.*, **49**, 1695 (1993).

Kissin, Y. V., *Isospecific Polymerization of Olefins with Heterogeneous Ziegler-Natta Catalysts*, Springer-Verlag, New York (1985).

Lorenzini, P., P. Bertrand, and J. Villermaux, "Modelling Ethylene and α-Olefin Copolymerization Using Ziegler-Natta Catalyst," *Can. J. Chem. Eng.*, **69**, 682 (1991).

Marques, M. M. V., C. P. Nunes, P. J. T. Tait, and A. R. Dias, "Polymerization of Ethylene Using a High-Activity Ziegler-Natta Catalyst. II. Molecular Weight Regulation," *J. Poly. Sci. Part A: Poly. Chem.*, **31**, 219 (1993).

McAuley, K. B., "Modeling, Estimation and Control of Product Properties in a Gas Phase Polyethylene Reactor," PhD Thesis, McMaster Univ., Hamilton, Ont., Canada (1991).

McAuley, K. B., J. F. MacGregor, and A. E. Hamielec, "A Kinetic Model for Industrial Gas-Phase Ethylene Copolymerization," *AIChE J.*, **36**, 837 (1990).

McAuley, K. B., J. P. Talbot, and T. J. Harris, "A Comparison of Two-Phase and Well-Mixed Models for Fluidized Bed Polyethylene Reactors," *Chem. Eng. Sci.*, **49**, 2035 (1994).
Payn, C. F., "Perspectives on the Commercial Direction of Metallocene Technology to 2000," *Metcon'93*, Houston (1993).
Ray, W. H., T. L. Douglas, and E. W. Godsalve, "Molecular Weight Distributions in Copolymer Systems. II. Free Radical Copolymerization," *Macromol.*, **4**, 166 (1971).
Salajka, Z., J. Kratochvila, P. Hudec, and P. Vecorek, "One-Phase Supported Titanium-Based Catalysts for Polymerization of Ethylene. II. Effect of Hydrogen," *J. Poly. Sci. Part A: Poly. Chem.*, **31**, 1493 (1993).
Short, J. N., "Low Pressure Ethylene Polymerization Processes," *Transition Metal Catalyzed Polymerizations Alkenes and Dienes*, R. P. Quirk, ed., Harwood, New York, p. 651 (1981).
Tait, P. J. T., and N. D. Watkins, "Monoalkene Polymerization: Mechanisms," *Comprehensive Polymer Science*, Vol. 4, G. C. Eastmond, A. Ledwith, S. Russo, and P. Sigwalt, eds., Pergamon, New York, p. 533 (1989).
Villermaux, J., P. Lorenzini, P. Bertrand, and J. L. Greffe, "Modelling of Polymerization of Ethylene by Ziegler-Natta Catalysis," *Polymer Reaction Engineering*, K. H. Reichert and W. Geiseler, eds., VCH Publishers, New York, 350 (1989).
Xie, T. Y., K. B. McAuley, C. C. Hsu, and D. W. Bacon, "Gas Phase Ethylene Polymerization: Production Processes, Polymer Properties, and Reactor Modelling," *Ind. Eng. Chem. Res.*, **33**, 449 (1994).
Xie, T. Y., and A. E. Hamielec, "Modelling Free Radical Copolymerization Kinetics: Evaluation of the Pseudo-Kinetic Rate Constant Method: I. Molecular Weight Calculations for Linear Copolymers," *Makromol. Chem. Theory Simulations*, **2**, 421 (1993a).
Xie, T. Y., and A. E. Hamielec, "Modelling Free Radical Copolymerization Kinetics: Evaluation of the Pseudo-Kinetic Rate Constant Method: II. Molecular Weight Calculations for Copolymers with Long Chain Branching," *Makromol. Chem. Theory Simulations*, **2**, 455 (1993b).
Xie, T. Y., and A. E. Hamielec, "Modelling Free Radical Copolymerization Kinetics: III. Molecular Weight Calculations for Copolymers with Crosslinking," *Makromol. Chem. Theory Simulations*, **2**, 777 (1993c).

Appendix: Moment Equations

The moment equations of live and dead polymer chain distributions are given as

$$\frac{d(Y_{10}(j)V)}{Vdt} = \frac{Y_{10}(j)_f V_f}{V} + R_{I1}(j) + R_{fm1}(j) + R_{iHA1}(j) + K_{21}(j)Y_{20}(j)[M_1] - \Big\{K_{12}(j)[M_2] + K_{f11}(j)[M_1] + K_{f12}(j)[M_2] + K_{fsp1}(j) + K_{fH1}(j)[H_2] + K_{fA1}(j)[A] + K_{dsp1}(j) + K_{dZ1}(j)[Z] + K_{dA1}(j)[A] + K_{dH1}(j)[H_2] + K_{d11}(j)[M_1] + K_{d12}(j)[M_2] + \frac{1}{\theta}\Big\}Y_{10}(j) \quad \text{(A1)}$$

$$\frac{d(Y_{20}(j)V)}{Vdt} = \frac{Y_{20}(j)_f V_f}{V} + R_{I2}(j) + R_{fm2}(j) + R_{iHA2}(j) + K_{12}(j)Y_{10}(j)[M_2] - \Big\{K_{21}(j)[M_1] + K_{f21}(j)[M_1] + K_{f22}(j)[M_2] + K_{fsp2}(j) + K_{fH2}(j)[H_2] + K_{fA2}(j)[A] + K_{dsp2}(j) + K_{dZ2}(j)[Z] + K_{dA2}(j)[A] + K_{dH2}(j)[H_2] + K_{d21}(j)[M_1] + K_{d22}(j)[M_2] + \frac{1}{\theta}\Big\}Y_{20}(j) \quad \text{(A2)}$$

$$\frac{d(Y_{11}(j)V)}{Vdt} = \frac{Y_{11}(j)_f V_f}{V} + M_1\{R_{I1}(j) + R_{fm1}(j) + R_{iHA1}(j)\} + K_{21}(j)Y_{21}(j)[M_1] + \{K_{11}(j)Y_{10}(j) + K_{21}(j)Y_{20}(j)\}M_1[M_1] - \Big\{K_{12}(j)[M_2] + K_{f11}(j)[M_1] + K_{f12}(j)[M_2] + K_{fsp1}(j) + K_{fH1}(j)[H_2] + K_{fA1}(j)[A] + K_{dsp1}(j) + K_{dZ1}(j)[Z] + K_{dA1}(j)[A] + K_{dH1}(j)[H_2] + K_{d11}(j)[M_1] + K_{d12}(j)[M_2] + \frac{1}{\theta}\Big\}Y_{11}(j) \quad \text{(A3)}$$

$$\frac{d(Y_{21}(j)V)}{Vdt} = \frac{Y_{21}(j)_f V_f}{V} + M_2\{R_{I2}(j) + R_{fm2}(j) + R_{iHA2}(j)\} + K_{12}(j)Y_{11}(j)[M_2] + \{K_{12}(j)Y_{10}(j) + K_{22}(j)Y_{20}(j)\}M_2[M_2] - \{K_{21}(j)[M_1] + K_{f21}(j)[M_1] + K_{f22}(j)[M_2] + K_{fsp2}(j) + K_{fH2}(j)[H_2] + K_{fA2}(j)[A] + K_{dsp2}(j) + K_{dZ2}(j)[Z] + K_{dA2}(j)[A] + K_{dH2}(j)[H_2] + K_{d21}(j)[M_1] + K_{d22}(j)[M_2] + \frac{1}{\theta}\Big\}Y_{21}(j) \quad \text{(A4)}$$

$$\frac{d(Y_{12}(j)V)}{Vdt} = \frac{V_{12}(j)_f V_f}{V} + M_1^2\{R_{I1}(j) + R_{fm1}(j) + R_{iHA1}(j)\} + K_{21}(j)Y_{22}(j)[M_1] + \{K_{11}(j)Y_{10}(j) + K_{21}(j)Y_{20}(j)\}M_1^2[M_1] + 2M_1[M_1]\{K_{11}(j)Y_{11}(j) + K_{21}(j)Y_{21}(j)\} - \Big\{K_{12}(j)[M_2] + K_{f11}(j)[M_1] + K_{f12}(j)[M_2] + K_{fsp1}(j) + K_{fH1}(j)[H_2] + K_{fA1}(j)[A] + K_{dsp1}(j) + K_{dZ1}(j)[Z] + K_{dA1}(j)[A] + K_{dH1}(j)[H_2] + K_{d11}(j)[M_1] + K_{d12}(j)[M_2] + \frac{1}{\theta}\Big\}Y_{12}(j) \quad \text{(A5)}$$

$$\frac{d(Y_{22}(j)V)}{Vdt} = \frac{Y_{22}(j)_f V_f}{V} + M_2^2\{R_{I2}(j) + R_{fm2}(j) + R_{iHA2}(j)\} + K_{12}(j)Y_{12}(j)[M_2] + \{K_{12}(j)Y_{10}(j) + K_{22}(j)Y_{20}(j)\}M_2^2[M_2] + 2M_2[M_2]\{K_{12}(j)Y_{11}(j) + K_{22}(j)Y_{21}(j)\} - \Big\{K_{21}(j)[M_1] + K_{f21}(j)[M_1] + K_{f22}(j)[M_2] + K_{fsp2}(j) + K_{fH2}(j)[H_2] + K_{fA2}(j)[A] + K_{dsp2}(j) + K_{dZ2}(j)[Z] + K_{dA2}(j)[A] + K_{dH2}(j)[H_2] + K_{d22}(j)[M_2] + K_{d21}(j)[M_1] + \frac{1}{\theta}\Big\}Y_{22}(j) \quad \text{(A6)}$$

$$\frac{d[Q_0(j)V]}{Vdt} = \frac{Q_0(j)_f V_f}{V} + \{K_{f11}(j)[M_1] + K_{f12}(j)[M_2] + K_{fH1}(j)[H_2] + K_{fA1}(j)[A] + K_{fsp1}(j) + K_{dz1}(j)[Z] + K_{dA1}(j)[A] + K_{dH1}(j)[H_2] + K_{d11}(j)[M_1] + K_{d12}(j)[M_2] + K_{dsp1}(j)\}Y_{10}(j) + \{K_{f21}(j)[M_1] + K_{f22}(j)[M_2] + K_{fH2}(j)[H_2] + K_{fA2}(j)[A] + K_{fsp2}(j) + K_{dz2}(j)[Z] + K_{dH2}(j)[H_2] + K_{dA2}(j)[A] + K_{d21}(j)[M_1] + K_{d22}(j)[M_2] + K_{dsp2}(j)\}Y_{20}(j) - \frac{Q_0(j)}{\theta} \quad \text{(A7)}$$

$$\frac{d[Q_1(j)V]}{Vdt} = \frac{Q_1(j)_f V_f}{V} + \{K_{f11}(j)[M_1] + K_{f12}(j)[M_2] + K_{fH1}(j)[H_2] + K_{fA1}(j)[A] + K_{fsp1}(j) + K_{dz1}(j)[Z] + K_{dA1}(j)[A] + K_{dH1}(j)[H_2] + K_{d11}(j)[M_1] + K_{d12}(j)[M_2] + K_{dsp1}(j)\}Y_{11}(j) + \{K_{f21}(j)[M_1] + K_{f22}(j)[M_2] + K_{fH2}(j)[H_2] + K_{fA2}(j)[A] + K_{fsp2}(j) + K_{dz2}(j)[Z] + K_{dH2}(j)[H_2] + K_{dA2}(j)[A] + K_{d21}(j)[M_1] + K_{d22}(j)[M_2] + K_{dsp2}(j)\}Y_{21}(j) - \frac{Q_1(j)}{\theta} \quad \text{(A8)}$$

$$\frac{d[Q_2(j)V]}{Vdt} = \frac{Q_2(j)_f V_f}{V} + \{K_{f11}(j)[M_1] + K_{f12}(j)[M_2] + K_{fH1}(j)[H_2] + K_{fA1}(j)[A] + K_{fsp1}(j) + K_{dz1}(j)[Z] + K_{dA1}(j)[A] + K_{dH1}(j)[H_2] + K_{d11}(j)[M_1] + K_{d12}(j)[M_2] + K_{dsp1}(j)\}Y_{12}(j) + \{K_{f21}(j)[M_1] + K_{f22}(j)[M_2] + K_{fH2}(j)[H_2] + K_{fA2}(j)[A] + K_{fsp2}(j) + K_{dz2}(j)[Z] + K_{dH2}(j)[H_2] + K_{dA2}(j)[A] + K_{d21}(j)[M_1] + K_{d22}(j)[M_2] + K_{dsp2}(j)\}Y_{22}(j) - \frac{Q_2(j)}{\theta} \quad \text{(A9)}$$

where

$$R_{fm1}(j) = [K_{f11}(j)Y_{10}(j) + K_{f21}(j)Y_{20}(j)][M_1]$$

$$R_{fm2}(j) = [K_{f12}(j)Y_{10}(j) + K_{f22}(j)Y_{20}(j)][M_2]$$

$$R_{iHA1}(j) = \{K_{iH1}(j)[P^*_{H,0}(j)] + K_{iA1}[P^*_{A,0}(j)]\}[M_1]$$

$$R_{iHA2}(j) = \{K_{iH2}(j)[P^*_{H,0}(j)] + K_{iA2}[P^*_{A,0}(j)]\}[M_2].$$

Manuscript received Feb. 28, 1994, and revision received May 16, 1994.